(Received 3 September 2024, Accepted 22 October 2024, Scheduled 26 October 2024)

Ultrawideband High-Gain Stacked Microstrip Antenna with Modified E-Shaped Active Exciter and Four Single-Sided Bowtie Passive Elements

Mikhail S. Shishkin*

Moscow Technical University of Communication and Informatics (Science and Research Department), Moscow, Russia

ABSTRACT: The article presents a method that allows for the high gain of a stacked microstrip antenna on an air substrate in an ultrawide frequency range. The method uses an active exciter in the form of a modified E-shaped patch, as well as four single-sided bowtie passive elements placed in the corners above the active one. The active element can match an antenna in an ultra-wide frequency range (up to 100%) with an impedance bandwidth matching of 10 dB or better, whereas passive elements are able to produce unidirectional radiation in the range of approximately 70–80% with a gain of more than 10 dBi. Based on the method under study, an ultrawideband antenna design was made which operates in a frequency band of 3,915 to 11,046 MHz (95.3%) with an impedance bandwidth matching of 10 dB and a bandwidth about 83% with $|S_{11}| \leq -15$ dB; the usable bandwidth with a gain of more than 10 dBi in the normal direction to the antenna plane with a cross-polar discrimination more than 55 dB is 77% (3,925–8,837 MHz). At frequencies below 4 GHz and above 9 GHz, the phase center shifts, and accordingly, the main lobe of the radiation pattern (radiation maximum) deflects. All antenna elements (one active and four passives) are made of sheet metal (e.g., stainless steel) and are connected to the conductive screen by steel or dielectric racks. The antenna dimensions are $1.05\lambda_{\max} \times 1.2\lambda_{\max} \times 0.1\lambda_{\max}$ $(1.7\lambda_0 \times 1.9\lambda_0 \times 0.2\lambda_0)$. Owing to its high performance, the antenna may be used as a measuring device in radio monitoring systems or in laboratories.

1. INTRODUCTION

As it is known, the 3.1–10.6 GHz frequency range is allocated by the Federal Communications Commission for ultrawideband (UWB) radio systems. In order to provide radio coverage over a small area, usually indoors or within the operational range of an object, such as a person or a machine, radio transmitting devices in this range are typically needed to run at low power [1]. Subsequently, several UWB antenna designs with an omnidirectional radiation pattern (RP) or a shape similar to omnidirectional one are being developed, as methods for designing such antennas. In particular, [2–13] illustrate that different frequency bands ranging from 40% to 80% or more can be potentially acquired with a matching level of more than 10 dB. Moreover, for the proposed antennas, there are methods for obtaining both one linear polarization [2–8] and two orthogonal ones, including circular [9–13]. The challenge of designing such antennas originates predominantly from the necessity to match the antenna across a very wide frequency range while simultaneously guaranteeing stable characteristics throughout this range, such as the shape of the radiation pattern and polarization (axial ratio).

In addition to the use of UWB antennas with an omnidirectional RP (or close to it), unidirectional antennas are often used, having a gain at least 9–10 dBi in an ultrawide frequency range. Such antennas are usually used as receiving antennas in radio monitoring systems or for measurement purposes (for example, as a measuring or reference antenna for measurements in an anechoic chamber). Among the antennas operating in an ultrawide range (more than 40%) with a unidirectional pattern and gain more than 9–10 dBi, one can distinguish the so-called Vivaldi antennas [14–23], logarithmic-periodic antennas (LPAs) [15, 16, 23–29], and horn antennas with a rectangular aperture shape (pyramidal horn) [15, 16, 23, 30–34]. These antennas include a number of drawbacks, including highly complicated designs, large sizes relative to the wavelength, and inconsistent gain over the operational range.

Aside from the common Vivaldi antennas, LPAs, and horn antennas, unidirectional UWB antennas with operating frequency bands of more than 40% and a gain of no more than 7–8 dBi are being designed and studied [35–39]. It has been established that combining several elements into an antenna array may boost the antenna gain. Fortunately, developing a feed network for such systems that would stimulate the elements with a suitable phase and amplitude distribution becomes incredibly complicated if the systems have ultrawide ranges [40–49].

The article presents an innovative technique for obtaining high gain in an ultrawide radio frequency range for a microstrip stacked antenna. This approach refers to the application of four passive single-sided bowtie elements at the corners above the active exciter, which is a modified E-shaped patch placed above a metal screen. The antenna manufactured using the proposed method operates in a frequency band of 3,915 to 11,046 MHz ($\sim 95\%$) with an impedance bandwidth matching of 10 dB; the antenna has a gain of more than 10 dBi in the frequency band

* Corresponding author: Mikhail S. Shishkin (mikkhail666@gmail.com).

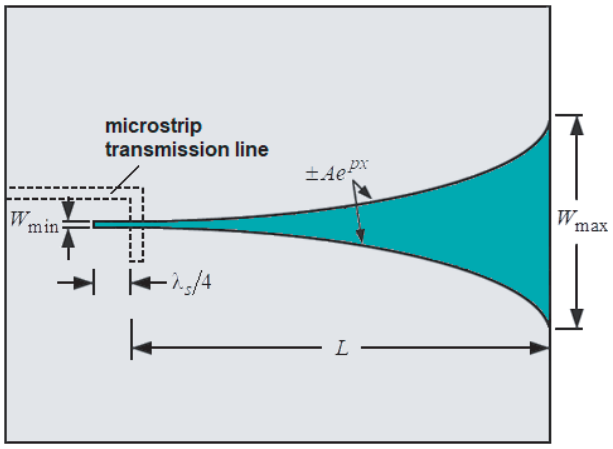

FIGURE 1. The basic geometry of a Vivaldi antenna.

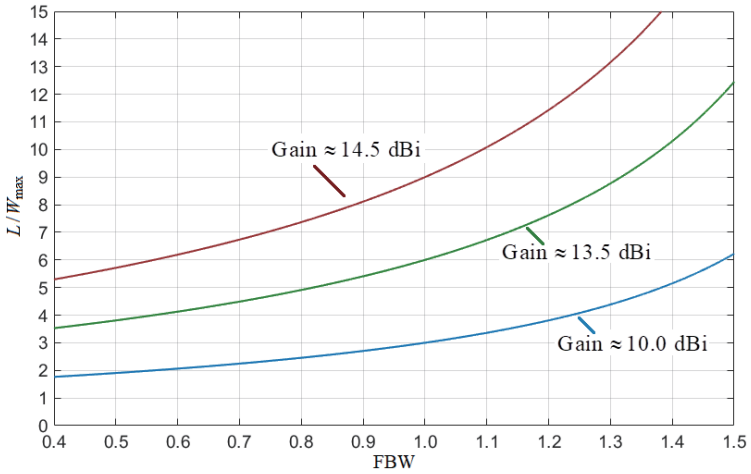

FIGURE 2. The relationship between Vivaldi antenna length and width depending on its gain and bandwidth.

of 3,925 to 8,837 MHz ($\sim$ 77%) in the normal direction to the antenna plane with cross-polar discrimination (XPD) of more than 55 dB. The antenna under study can be used as a measuring device in radio monitoring systems or in laboratories.

2. THE UWB HIGH-GAIN ANTENNA TECHNIQUES OVERVIEW

In terms of antenna technologies, let us propose the concept of "ultra-wideband." According to [1], on the one hand, the frequency range from 3.1 to 10.6 GHz is allocated for UWB systems. On the other hand, from the perspective of signal theory, a system is considered UWB where the signal must at any time have a fractional bandwidth (FBW) equal to or greater than 20% or have a bandwidth of 500 MHz regardless of the FBW [16, 23]. Antenna technology is not covered by either term in its whole. According to [50, 51], a wideband (or broadband) antenna is an antenna whose operating bandwidth exceeds 10%; obviously, the operating bandwidth of the UWB antenna should greatly exceed this value. A variety of authors [16–49] define UWB antennas as those whose lower limit of the operating frequency band which varies from 25% to 40%; this means that some authors classify UWB antennas as having an operating range of more than 25%, while others range from 40% and higher. Based on the above definitions and taking into account Kotelnikov's theorem, we will further assume that UWB includes antennas with an operating range of more than 40%, where:

$$\mathrm{BW} = \frac{f_u - f_l}{f_c} \cdot 100\% = 2 \cdot \frac{f_u - f_l}{f_u + f_l} \cdot 100\%, \qquad (1)$$

where f_u is the upper frequency of the operating range; f_l is the lower frequency of the operating range; f_c is the central frequency of the operating range.

The largest number of antennas operating in an ultrawide frequency range are designed to meet the requirements of [1], i.e., they operate in the range of 3.1–10.6 GHz at a low signal power level at the input with an omnidirectional RP. These antennas are exemplified in [2–13]. In the general run of things, the antennas are similar to each other in their design and operating principle and consist of printed UWB elements of various shapes, fed by a microstrip transmission line. It is illogical to combine such antennas into an array in order to increase directivity. In this regard, unidirectional UWB antennas are vital to consider for high gain applications.

2.1. Vivaldi Antenna and Its Modifications

The Vivaldi antenna is a wideband tapered slot antenna with an exponentially tapered profile, first introduced by Gibson in 1979 [14]. The basic geometry of the antenna is shown in Figure 1. The design consists of a slot of size $\lambda_s/4$, which expands exponentially to a size of $W_{\max}$. The slot is excited by a microstrip transmission line coming from the bottom surface of the substrate. An alternative Vivaldi antenna design uses a square or circular resonant region instead of a $\lambda_s/4$ slot, which is also excited by a microstrip transmission line. Due to the printed design in the Vivaldi antenna, it is possible to achieve high dimensional accuracy in its manufacture, while the antenna has a low cost. Obtaining high directivity (or high gain) in the antenna is achieved by increasing the length L of the antenna.

The bandwidth of such an antenna is limited by the width $W_{\min}$ and the aperture width $W_{\max}$ of the antenna. For the most effective radiation, according to [15, 16], the antenna length L must exceed one wavelength $\lambda_{\max}$ at the lowest frequency f_l of the operating range:

$$L > \lambda_{\max} = c/f_l. \qquad (2)$$

An increase in antenna gain is achieved by increasing its length L, so, for example, to achieve a gain of approximately 10 dBi, the antenna length $L = \lambda_{\max}$ is sufficient; to achieve a gain of 14.5 dBi, the antenna length should be approximately $3\lambda_{\max}$ [15, 16]. The value of the aperture width $W_{\max}$ should be in the range between $W_{\max 1}$ and $W_{\max 2}$, where:

$$W_{\max 1} \approx \lambda_0 = \frac{c}{f_c}, \qquad (3)$$

$$W_{\max 2} \approx \frac{\lambda_{\min}}{2} = \frac{c}{2 \cdot f_u}. \quad (4)$$

From (2)–(4) it can be seen that the wider the operating range of the Vivaldi antenna is, the higher the relationship is between its length L and width W, which can be seen in Figure 2.

Thus, a UWB Vivaldi antenna with a max gain about 15 dBi should have a length of more than $3\lambda_{\max}$, while its dimension ratio will be at least $6 : 1$ and higher for a wider operating frequency range. The main drawback of such an antenna is that its design would be highly fragile in terms of its application.

Based on the classical geometry of the Vivaldi antenna, a large number of different designs have been developed, and the authors were able to improve the performance of the antenna. For example, [17] discusses antipodal Vivaldi antenna (AVA) designs. The advantage of such antennas compared to the classical topology is an increase in gain and, as a result, an increase in efficiency; nevertheless, the maximum gain of such designs rarely exceeds 10–11 dBi. Gains of more than 10 dBi were achieved with Vivaldi antennas with different corrugation structures [17–21]. Thus, the authors, according to a study from [17], managed to achieve an antenna max gain of more than 15 dBi, and some corrugated AVAs have gain up to 18–20 dBi in an ultrawide frequency range. It is worth noting that not all designs provide stable efficiency over the entire operating frequency range, and the dimensions of such antennas often exceed $5\lambda_0$ or more, up to $10\lambda_0$. In [22], the authors were able to achieve a Vivaldi antenna gain of 9 to 15 dBi in the frequency range of more than 100% by combining two elements and placing them on a flexible substrate. Despite the high performance, the main disadvantage of the antenna is still its large size, so the length of the antenna is about $5\lambda_0$.

2.2. Logarithmic-Periodic Antennas

Log-periodic dipole array (LPDA) antennas were introduced and became widespread in the late 1950s. It is the first frequency-independent type of antenna [15, 23]. The LPDA consists of two in-plane sets of crisscrossed monopoles whose lengths and separations are related via the growth rate τ, as shown in Figure 3. The length of the first element depends on the minimum wavelength $\lambda_{\min}$ of the required operating frequency range:

$$l_{\min} = 0.3 \cdot \lambda_{\min} = 0.3 \cdot c/f_u. \quad (5)$$

The last, largest element is calculated based on the maximum wavelength $\lambda_{\max}$ of the required frequency range:

$$l_{\max} = 0.5 \cdot \lambda_{\max} = 0.5 \cdot c/f_l. \quad (6)$$

The distance between the largest element and the next one is calculated by the equation:

$$S_1 = \sigma \cdot \lambda_{\max}, \quad (7)$$

then the distances between the elements are equal:

$$S_n = S_1 \cdot \tau^{n-1}, \quad (8)$$

where the spacing factor σ can be founded from Figure 4.

Analyzing all the above, we can conclude that to achieve a gain of more than 10 dBi, the value of τ should be about 0.95,

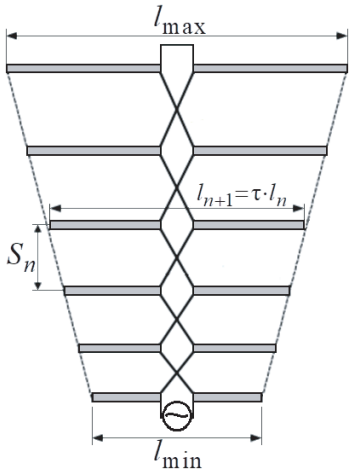

FIGURE 3. The basic geometry of a LPDA.

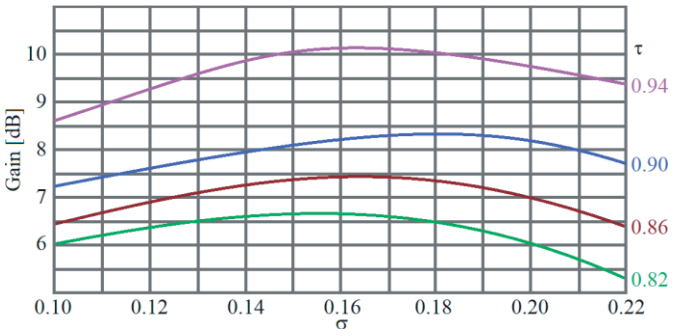

FIGURE 4. The relationship between τ and σ of an LPDA.

with the optimal value of σ being approximately 0.16–0.18. Then, a log-periodic dipole array antenna with an operating bandwidth of at least 50% must at least have a length of more than $3\lambda_0$ and consist of at least 19–20 elements. It is evident that such a design is highly difficult from both the manufacturing and application viewpoints.

There are a large number of modifications of log-periodic antennas, most often developed on the basis of printing technologies, where elements take on very different shapes, from bowtie-shaped to fractal structures [24–28], combining into a single system, as presented in [29]. These designs make it possible to expand the frequency range of the antenna, up to 100% or more, while reducing its size. Yet, all the antennas considered do not allow obtaining a maximum gain of more than 10 dBi, which determines their main drawback.

2.3. UWB Pyramidal Horn Antennas

The description, basic principles of operation, and types of horn antennas are given in sufficient detail in [15, 16, 23]. Horn antennas themselves are not ultra-wideband or even wideband. Despite the possibility of achieving high gain, the disadvantages of such antennas include their large size, poor cross-polar discrimination, and differences in the width of the main lobe of the radiation pattern in the two main planes.

There are designs of horn antennas with a gain of more than 10 dBi and having operating bands in an ultrawide frequency range, sometimes exceeding 100%. For example, in [30], a

modification of a pyramidal horn antenna was proposed, which made it possible to obtain a symmetrical pattern in two planes with a gain of 12–14 dBi and a bandwidth of about 89%. Basically, the ability to operate a horn antenna in an ultra-wide range is ensured through the use of a ridge. The authors in [31–33] demonstrate the possibilities of expanding the operating frequency range with high gain using ridged horn antennas with metallic grid sidewalls. Such designs make it possible to obtain an operating frequency bandwidth much higher than 100% (180% in [32] and 167% in [33]), while the antenna gain ranges from 10 to 18 dBi, growing progressively as the operating frequency increases. In [34], the authors additionally use a lens, which improves the gain uniformity across the frequency band.

Among the disadvantages of the UWB horn antennas considered, we can highlight: differences in the width of the RP in the main planes [31, 32], shift of the maximum; bifurcation of the main lobe [32–34], low XPD, large sizes ($7.6\lambda_0 \times 5\lambda_0 \times 8.5\lambda_0$ in [31], $4.8\lambda_0 \times 3.3\lambda_0 \times 11.6\lambda_0$ in [32], $8.1\lambda_0 \times 4\lambda_0 \times 3.5\lambda_0$ in [33], $6\lambda_0 \times 4.5\lambda_0 \times 8.4\lambda_0$ in [34]), heavy weight of the antenna (on average from 0.5 to 1.5 kg), requirements for high precision manufacturing of all antenna elements, and high manufacturing cost.

2.4. Other UWB Unidirectional Antennas

Besides the most common UWB antennas, such as Vivaldi antennas, pyramidal horn antennas, LPDAs, and their modifications, there are various unidirectional UWB antennas with a low gain (on average no more than 7–8 dBi). Therefore, for example, in [35], a construction composed of a planar electric dipole and a shorted patch antenna is given. The antenna has a matching bandwidth of about 44% with a gain of 7 to 8 dBi in the operating range. In [36], the author presents an antenna that has the semblance of LPA based on broadband printed elements. The antenna provides a wide impedance bandwidth of 103% and a usable bandwidth of 84% and has a gain of 4 to 7 dBi in the working frequency band. In [37], the authors present a printed horn with significantly smaller dimensions compared to a classical pyramidal horn. Moreover, such an antenna is much easier to manufacture. A low level of matching (around 6 dB) and a low gain (about between 2.5 and 8 dBi in the operating frequency band) serve as two of the antenna's drawbacks.

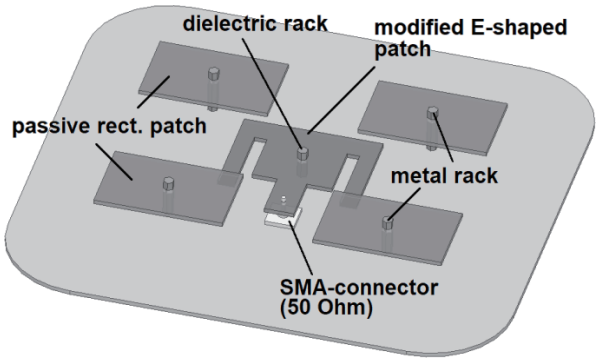

FIGURE 5. A modified E-shaped patch for UWB high-gain stacked microstrip antenna.

The authors from [38] and [39], where designs of UWB unidirectional antennas with circular polarization were presented, were able to achieve high performance. The antennas have impedance matching bandwidths of 71% [38] and 125% [39], while the axial-ratio bandwidths are 50% [38] and 120% [39]. Both antennas have a stable form of RP throughout the entire operating frequency range; the measured antenna gain in [38] is 8.7 dBi and is stable throughout the entire operating range; in [39], the measured gain varies from 6 to 12 dBi, and the average gain is about 9 dBi.

There are various modifications of UWB antenna arrays, both in-phase and with scanning capabilities [40–49]. As is known, combining several elements into a single system can significantly improve the directivity of the antenna; however, in an ultrawide frequency range, this approach has a number of disadvantages. In particular, it is rarely possible to achieve a stable shape of the RP throughout the entire operating range since the distance (relative to the wavelength) between the elements varies greatly depending on the frequency; in addition, the feed network in the UWB range is difficult to implement, and depending on frequencies within the operating range, it can introduce phase and amplitude distortions into the shoulders.

Thus, by using an antenna array, we significantly increase the size of the antenna, but it is not always possible to achieve high performance. For example, in [41], a 2×4 array with a bandwidth of about 57% was proposed, while the average gain that the authors managed to achieve was only 13.2 dBi. A similar situation is observed in [44], where a 4×4 array is proposed ($4.5\lambda_0 \times 3.8\lambda_0 \times 0.05\lambda_0$); the antenna radiation efficiency in the operating range varies from 26% to 72%, while a shift of the main lobe is observed on some frequencies without scanning.

In this regard, we can judge that the development and research of new types of antennas with a simple design capable of providing high performance in an ultrawide frequency range is a crucial and up-to-date issue.

3. THE UWB HIGH-GAIN STACKED MICROSTRIP ANTENNA DESCRIPTION

Many resources are devoted to wideband microstrip antennas based on the use of passive elements jointly active ones. Examples of such designs can be found in [15, 16, 23, 50–52], where it was possible to achieve a unidirectional antenna bandwidth of more than 30% with stable performance in the operating range. In [53], a stacked microstrip antenna was studied, resulting in a design with a matching bandwidth of 33% at a level of $|S_{11}| < 10$ dB with a gain of more than 10 dBi. In [53], in the classical antenna presented in [54], the active exciter was replaced with a wider-bandwidth E-shaped patch, which made it possible to significantly improve the performance of the antenna. However, the results achieved in [53] and the conclusions obtained give reason to believe that the performance of the proposed antenna can be significantly improved.

3.1. Active Exciter Bandwidth Enhancement

In [53], the possibility of expanding the operating bandwidth of a stacked microstrip antenna through the use of an E-shaped

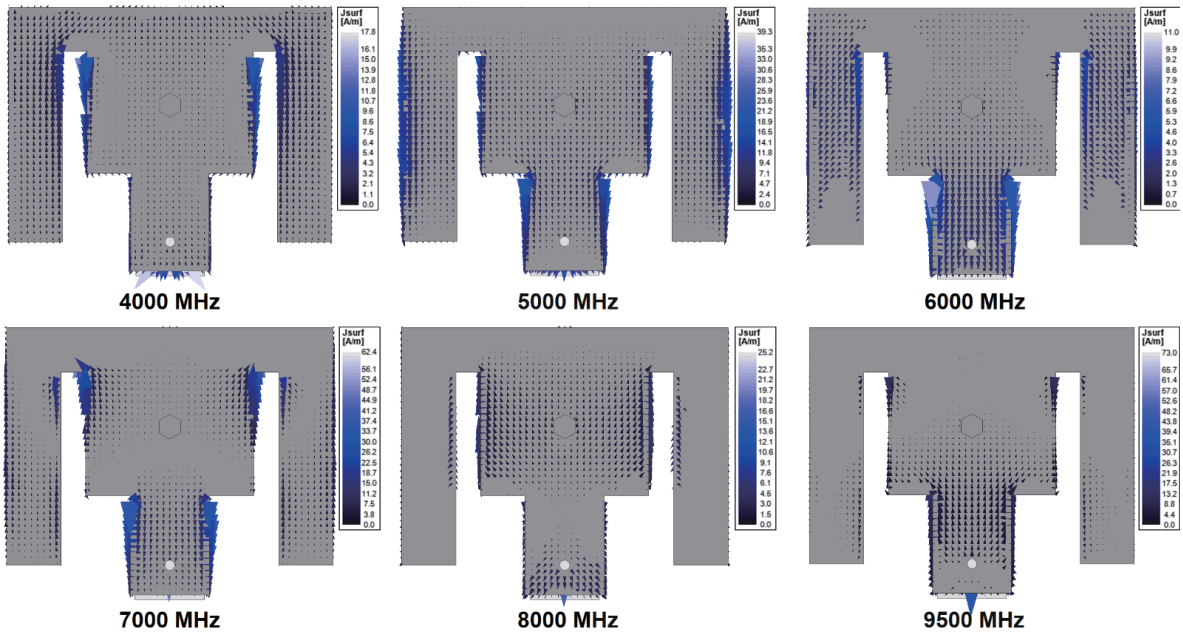

FIGURE 6. The current distribution on the surface of the modified E-shaped active exciter.

active exciter, which is described in many papers, for example [15, 16, 23], was demonstrated. Yet, there are a large number of modifications of E-shaped antennas where the authors were able to significantly expand their operating bandwidth [55–57]. Thus, it is suggested to replace the active exciter in the design proposed in [53] with a wider-bandwidth one, as given in Figure 5. Firstly, the arms of the patch have become longer, and the dimensions of the cutouts have changed. Secondly, the rectangular design of the central element has been replaced by a symmetrical step in width where, following the example from [58], by shifting the power point, it is possible to achieve the desired matching in the required frequency range.

Previously, variants of equivalent circuits of a conventional E-shaped exciter were proposed [56, 59–61]; in the simplest case, the E-shaped patch is considered as two LC resonant circuits, the first of which is tuned to the frequency of the middle element (high frequency), the second at the frequency of a rectangular exciter, the size of which is equal to the size of the patch itself (low frequency).

If we consider the proposed modified E-shaped exciter, it consists of three parts: the first part is the smallest in size, to which the coaxial connector is directly connected, expanding into a wider part by symmetrical step, which is connected through a T-junction to the outer arms of the exciters.

Figure 6 shows the current distribution on the exciter surface at different frequencies. The current distribution calculation was performed in ANSYS EM Suite software without taking into account the influence of passive elements. It can be noticed that three resonant frequencies are being distinguished:

- in the frequency region of 5000 MHz, surface currents are concentrated on the edge of the largest rectangle, that is, the exciter itself;
- in the 8000 MHz frequency region, currents are concentrated at the edges of the larger center part;
- in the frequency region of 9500 MHz, currents are concentrated at the edge of the smallest center rectangular element of the exciter under consideration.

The mechanism for expanding the antenna's bandwidth can be shown as follows: as in the classical E-shaped antenna, the largest part can be considered as an LC resonant circuit with a frequency corresponding to the frequency of a similar rectangular microstrip antenna (with a resonant size of about $\lambda/2$); however, in the proposed exciter, the central part is not a single, but two resonant circuits, designed for frequencies in accordance with their sizes.

For understanding the principle of antenna operation, a diagram is presented in Figure 7. The left part shows the transformation of a conventional rectangular microstrip antenna into the proposed modified E-shaped exciter, where the central part is stepped with a transition from a narrower element to a wider one. The middle part shows the equivalent circuits of the antenna in the process of its transformation. The right side shows the reflection coefficient (absolute S_{11}) plots calculated for sequential LC circuits, each tuned to its own resonant frequency, approximately corresponding to the element size of the presented E-shaped exciter.

If we look at the bottom plot in Figure 7, we can see that three successive LC circuits correspondingly form resonances in the $|S_{11}|$ plot; it is determined by the smallest amplitude values (three reductions corresponding to three frequencies). However, for such circuits, a single matching band is not formed, and, in fact, such a circuit is multi-band rather than ultrawideband. For an antenna, such a plot will be smoother due to the

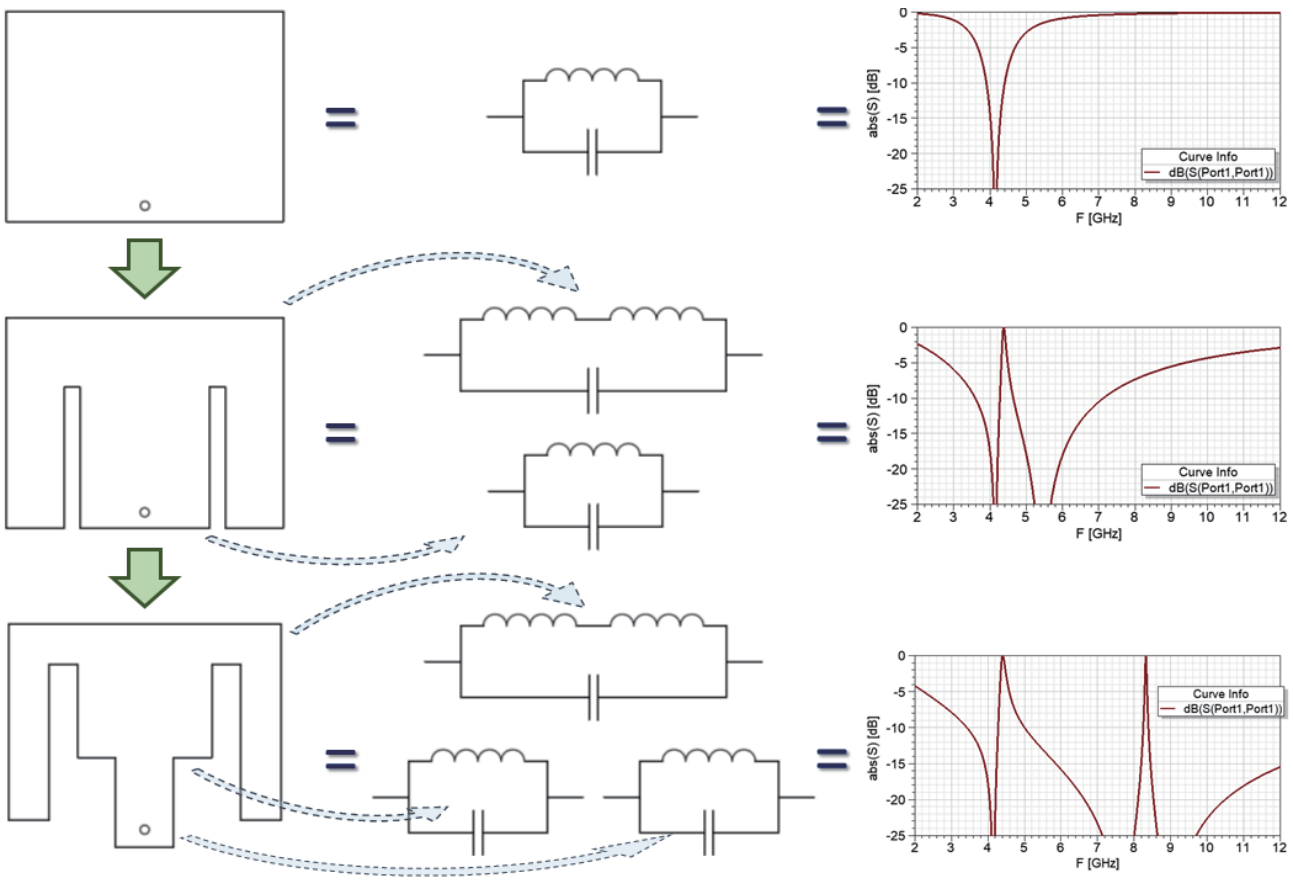

FIGURE 7. The wideband mechanism of the proposed modified E-shaped exciter.

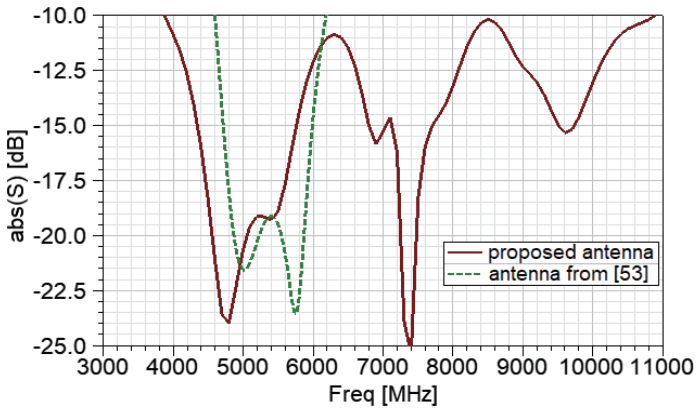

FIGURE 8. The simulated reflection coefficient magnitude of the stacked microstrip antenna with a modified E-shaped active exciter and four rectangular passive elements.

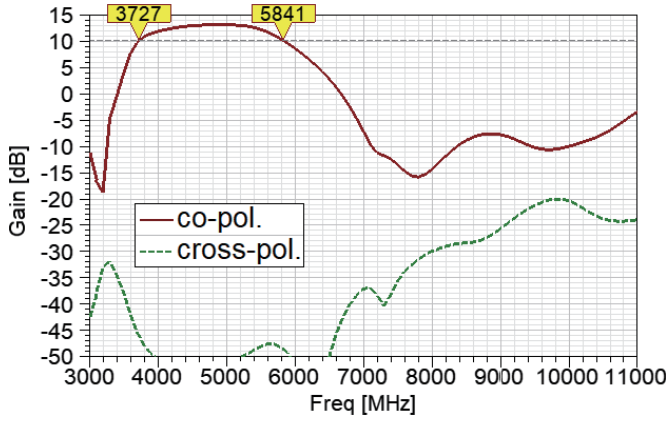

FIGURE 9. The simulated gain plot of the stacked microstrip antenna with a modified E-shaped active exciter and four rectangular passive elements.

fact that there is a coupling between the three main patch elements, as shown in Figure 8.

Figure 8 demonstrates the correspondence with the behavior of the $|S_{11}|$ plots predicted in Figure 7, that is, for a conventional E-shaped exciter we see two resonances, for the proposed modified one, three resonances. At the same time, due to the coupling between the patch elements, the plot is smoothed, forming a single matching band in an ultrawide frequency range. When designing a proposed antenna, one should consider the influence of passive elements on the active one, leading to the need to reduce the size of the last.

Figure 9 shows the antenna simulated gain plot. It can be noted that, in comparison with [53], the antenna bandwidth at the matching level of 10 dB has increased significantly (95% versus 33% from [53]). However, from the plot in Figure 9, it is clear that the antenna gain exceeds 10 dBi in a significantly

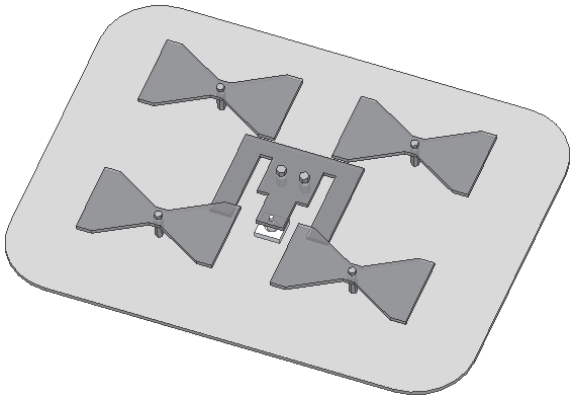

FIGURE 10. Stacked microstrip antenna with a modified E-shaped active exciter and four bowtie passive elements.

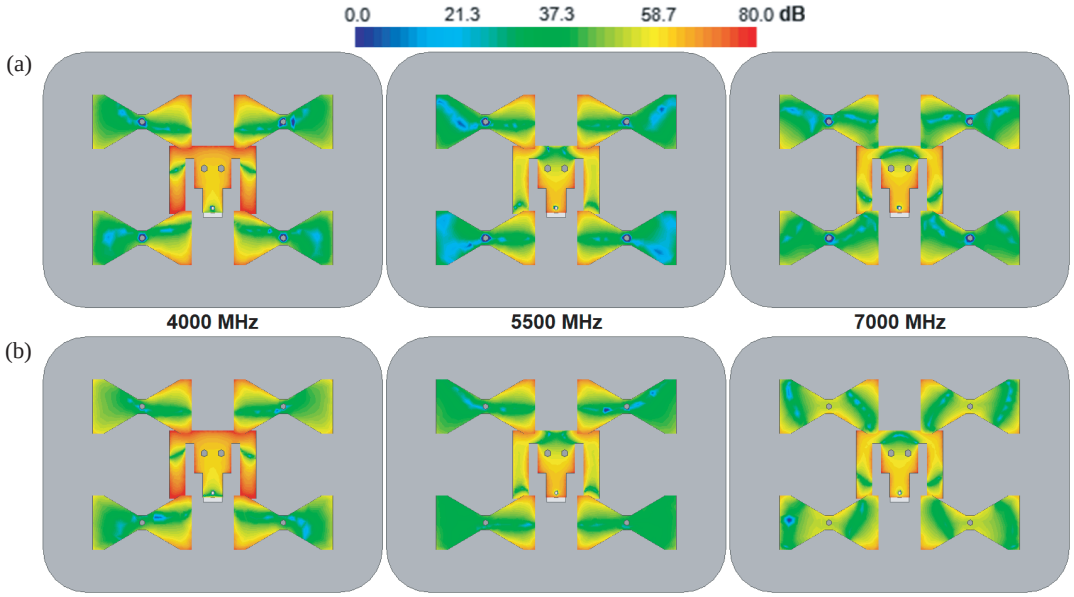

FIGURE 11. The E-field distribution on the surfaces of stacked microstrip antenna elements ((a) passive elements are on metal racks, (b) passive elements are on dielectric racks).

smaller band and is only 44% (3,727–5,841 MHz), which approximately corresponds to the results from [53], from which we can conclude that it is also necessary to modify passive antenna elements.

3.2. Passive Element Modifications

To replace passive rectangular exciters, bowtie elements are being considered, which are often used in wideband and ultrawideband antennas [62–64]. Figure 10 shows an example of such an antenna, where four passive bowtie patches are used. The sizes of the bowtie element correspond to the sizes of a rectangular element with a size designed for the lower part of the operating frequency range of the antenna; the element narrows towards the center. In the center of the element, a rack (metal or dielectric) is supposed to be installed to mount the element to the ground plane.

Figure 11 shows the E-field distribution on the surfaces of the elements of the proposed antenna with four passive bowtie elements. It can be noticed that the main part of the E-field is concentrated on half of the passive exciter, directed inside the antenna; the second part does not participate in the formation of the electromagnetic field. It follows that it is permissible to replace the passive bowtie element with a single-sided one. At the same time, the use of metal racks ensures both the strength of the structure and a more uniform field distribution among the passive elements.

Figure 12 shows the evolution of the passive elements of the proposed antenna and a comparison of this process with the resulting characteristics. At the first stage, the rectangular elements are replaced with a bowtie; then the bowties change to single-sided (which in turn significantly reduces the antenna area); rectangles are added to the passive elements, with the help of which it is possible to optimize the antenna matching. The last step is to replace the single-sided bowties with ring single-sided bowties.

From the results given in this section, it can be seen that, firstly, the impedance matching bandwidth of the antenna can

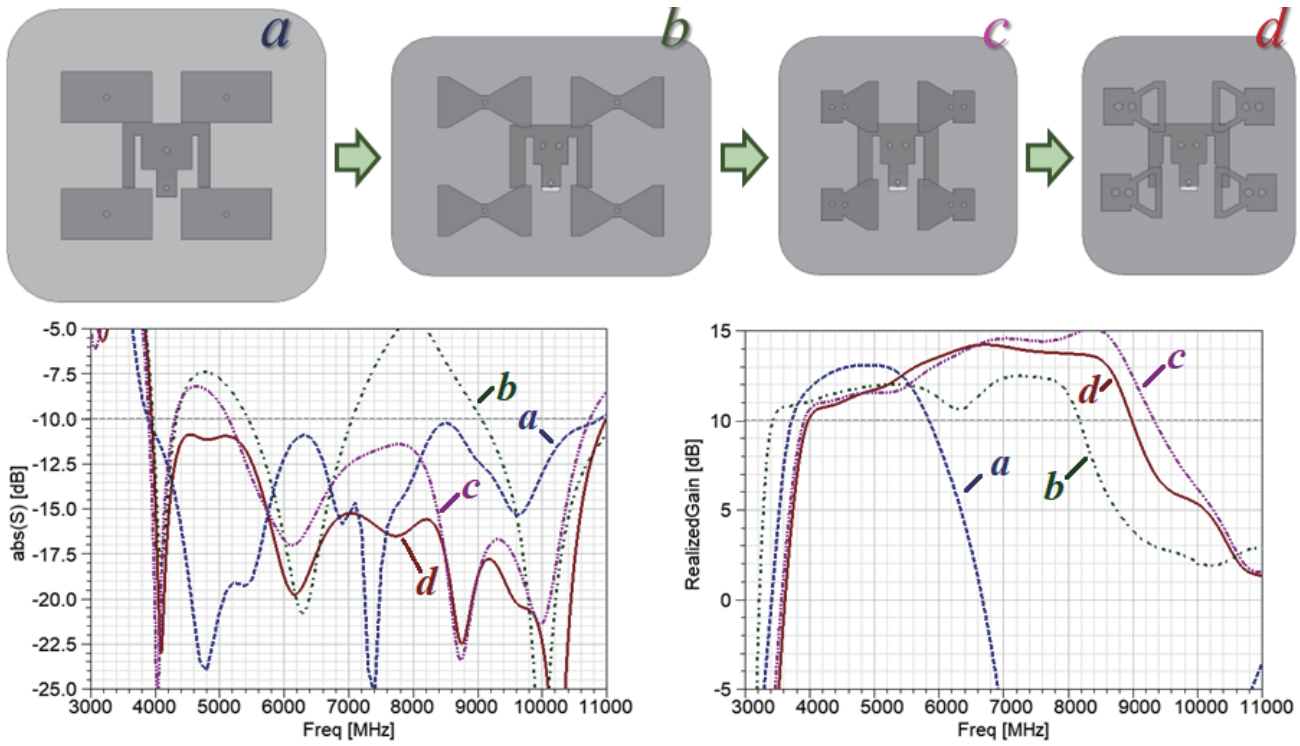

FIGURE 12. The evolution of the passive elements of the proposed stacked microstrip antenna (using only metal racks to mount passive elements).

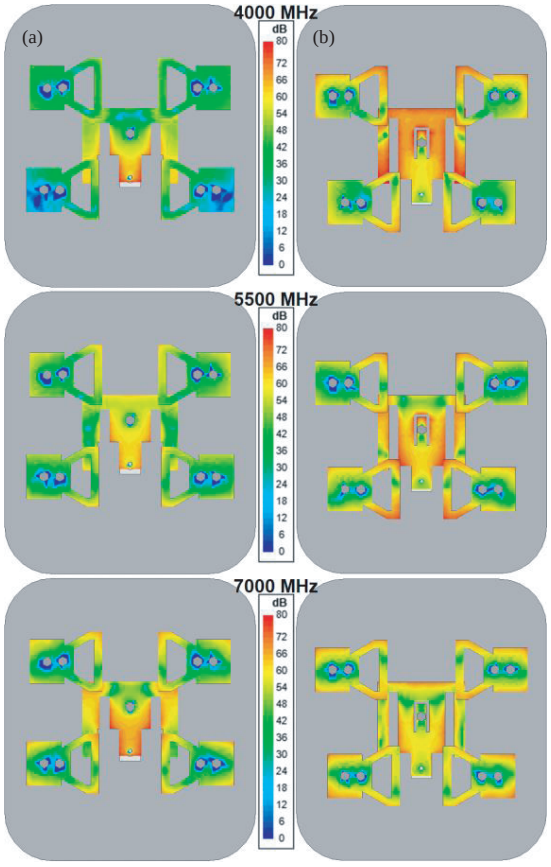

FIGURE 13. The E-field distribution on the antenna element surfaces with an E-shaped active exciter mounted (a) with metal rack having U-shaped isolating slot and (b) without it .

be considerably expanded by using a more wideband (ultra-wideband) active exciter; secondly, the antenna bandwidth in terms of gain level can be expanded by using wideband (ultra-wideband) passive elements. This article considers an E-shaped modified exciter as an active one and single-sided bowtie elements as passive ones.

3.3. Active Exciter with Metal Rack

In [50] and [65], it was proposed to use metal racks to mount the exciters, placing them in the center of the element (circular or rectangular) at the point of zero potential. Nevertheless, results in [53] showed that for an E-shaped patch, the use of a metal rack has an effect on the radiation characteristics, resulting in a shift in the maximum of the RP. To reduce the influence of the metal rack, an additional modification of the active E-shaped exciter is proposed by adding a U-shaped slot cut around the installation point of the rack.

Since the presence of a short-circuiting element generally changes the wave impedance of the active exciter, as shown, for example, in [15, 16], then, besides the addition of a U-shaped slot around the place where the metal rack is attached, the dimensions of the exciter itself, or more precisely its internal components, also change. Figures 13 and 14 show the E-field distribution on the antenna elements and the antenna gain patterns when using a metal rack to mount E-shaped patch. As can be seen from presented Figures, the U-slot provides isolation of the rack and equalization of currents (E-field) on the surface of the exciter and antenna respectively.

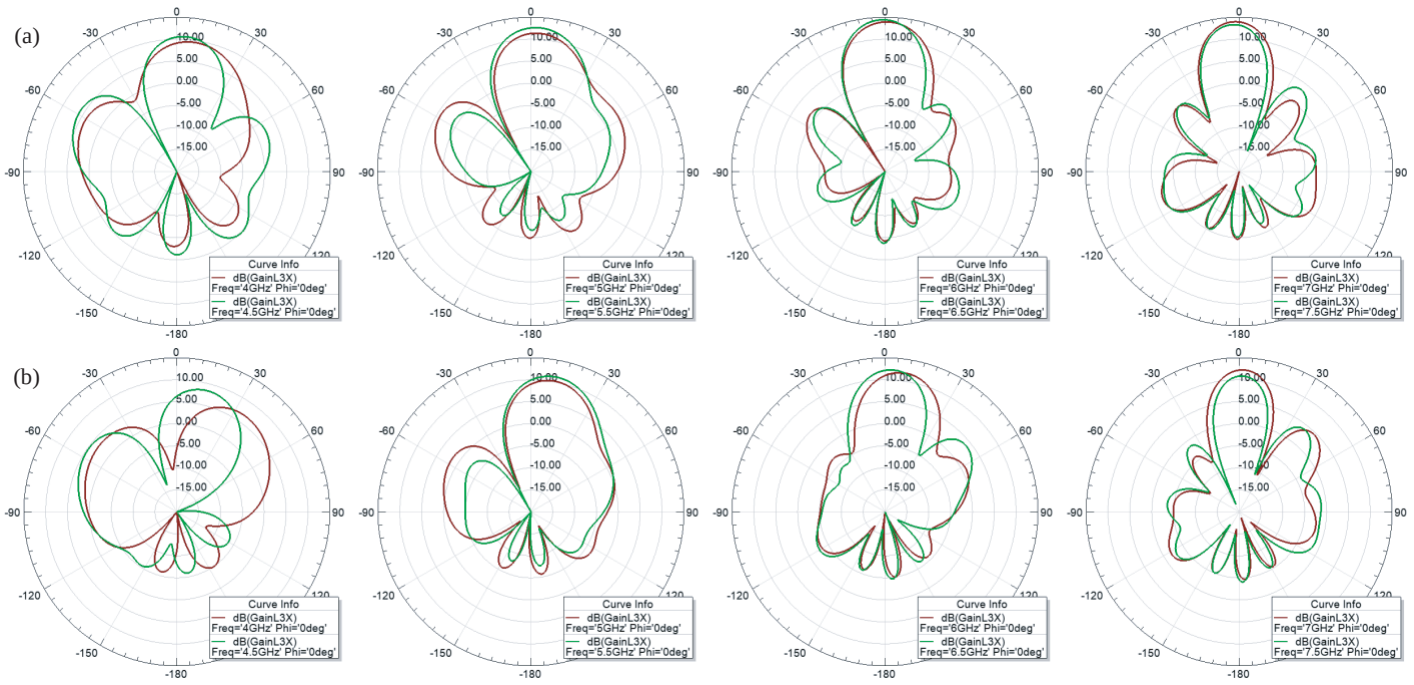

FIGURE 14. The XZ-gain patterns of the proposed stacked microstrip antenna (a) with using of a metal rack to mount the active modified E-shaped exciter having U-shaped isolating slot and (b) without it.

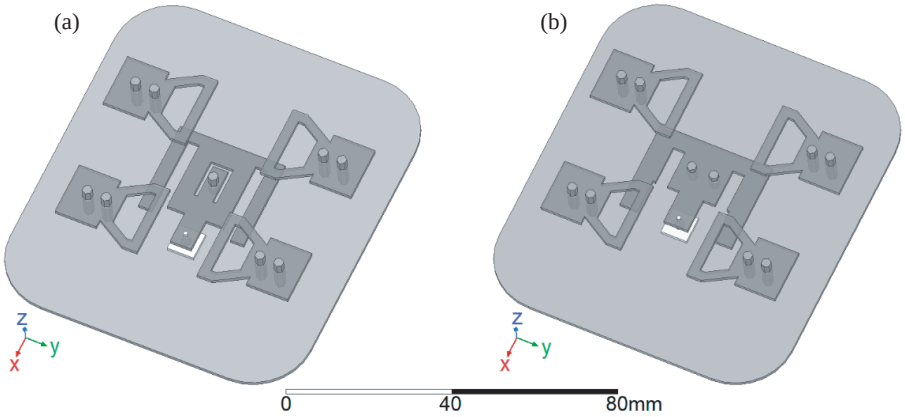

FIGURE 15. The models of the proposed UWB stacked microstrip antenna with four single-sided bowtie passive elements and a modified E-shaped active exciter mounted with a (a) metal rack and (b) dielectric racks.

4. THE UWB HIGH-GAIN STACKED MICROSTRIP ANTENNA SIMULATION RESULTS

This section contains comprehensive simulation results of two antenna variants (Figure 15), whose designs were obtained through optimization in the ANSYS EM Suite software (Figures 16–17). The first version of the antenna involves mounting an active exciter with a metal rack; the second involves dielectric ones. Both variants allow for passive elements to be mounted on metal racks.

From the simulation results, we can see that the antenna, where the active exciter is mounted using a metal rack, has a matching band of 77% (3,952–8,884 MHz) with $|S_{11}| \leq -10$ dB and about 45% with $|S_{11}| \leq -15$ dB; the usable antenna BW (with a gain of more than 10 dBi) is 4,131–8,105 MHz (65%) with XPD greater than 60 dB; the peak gain is 14.2 dBi at 6,445 MHz. An antenna where dielectric racks are used to mount an active exciter has better performance: the matching BW is 94.3% (3,947–10,991 MHz) with $|S_{11}| \leq -10$ dB and about 60% with $|S_{11}| \leq -15$ dB; the usable BW is 3,925–8,837 MHz (77%) with XPD greater than 55 dB; the peak gain is 13.85 dBi at 6,655 MHz; and the front-to-back ratio (FBR) is more than 17 dB at frequencies higher than 4.5 GHz. The antenna size, excluding the connector, is $80 \times 90 \times 10$ mm^3, which corresponds to $1.05\lambda_{\max} \times 1.2\lambda_{\max} \times 0.1\lambda_{\max}$ or $1.7\lambda_0 \times 1.9\lambda_0 \times 0.2\lambda_0$. At frequencies below 4 GHz and above 9 GHz, the phase center in both types of antennas shifts, and, accordingly, the main lobe of the radiation pattern (radiation maximum) deflects. The RPs of an antenna with a dielectric rack are more stable in the working band.

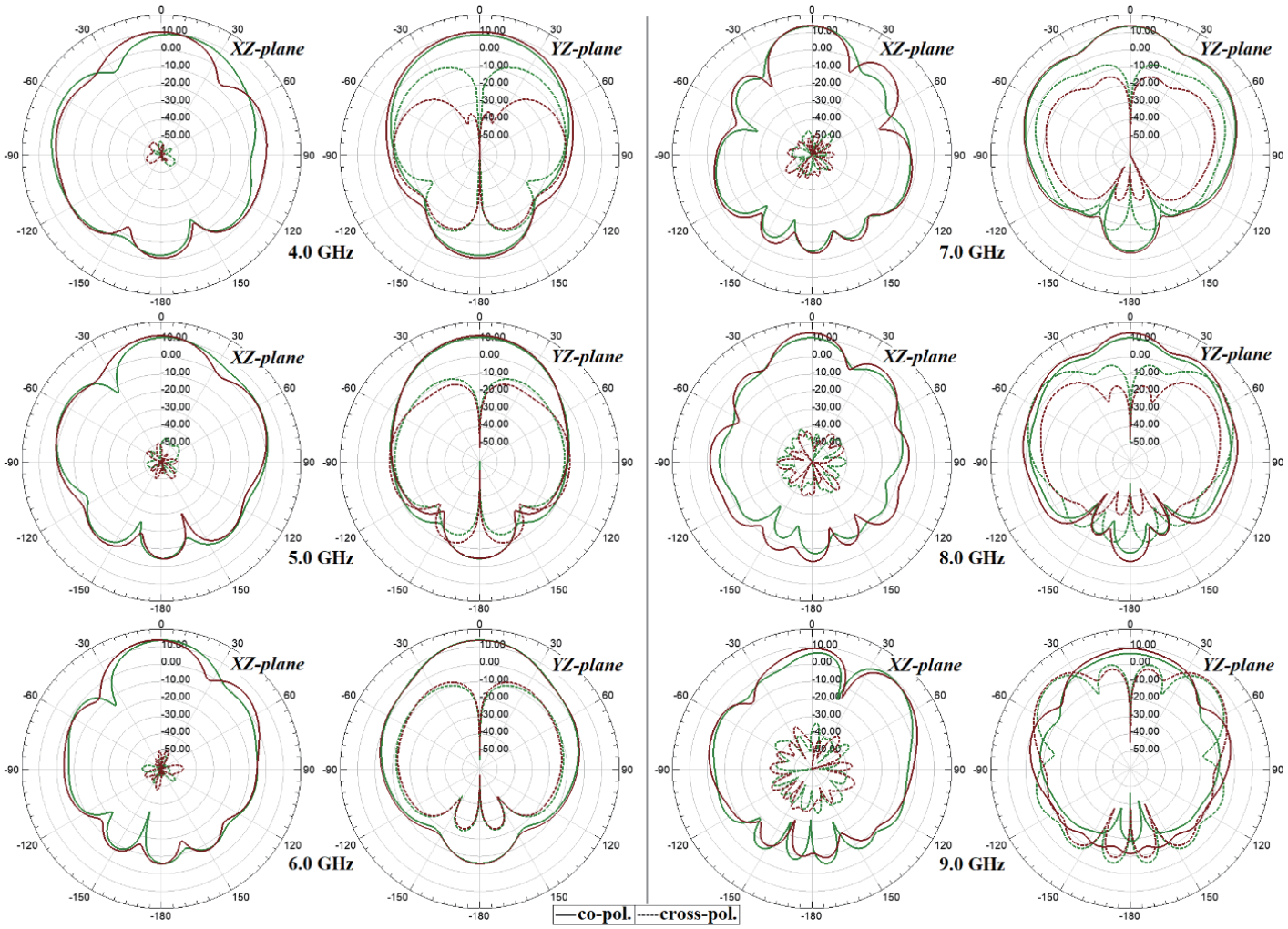

FIGURE 16. The simulated gain patterns of the proposed ultrawideband stacked microstrip antennas with a modified E-shaped active exciter mounted with a metal rack (*green*) and dielectric racks (*red*).

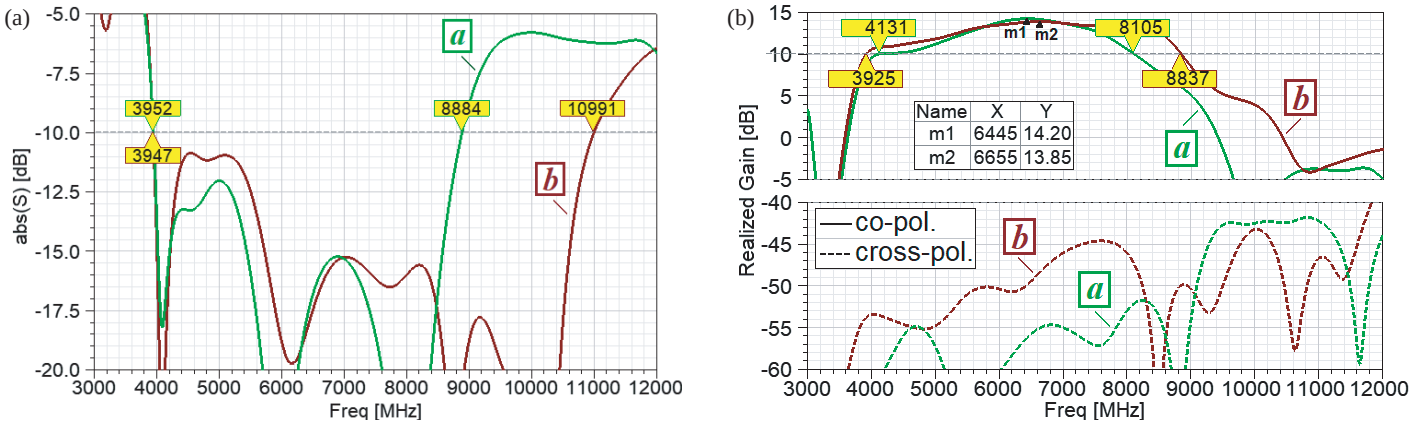

FIGURE 17. (a) The simulated reflection coefficient magnitudes and (b) the simulated realized gain plots of the stacked microstrip antennas with a modified E-shaped active exciter mounted with a metal rack (*a*) and dielectric racks (*b*).

5. THE UWB HIGH-GAIN STACKED MICROSTRIP ANTENNA EXPERIMENTAL RESULTS

The manufactured antennas are shown in Figure 18. The antenna elements (active, passives, and ground plane) are made of stainless steel sheets 1 mm thick using laser cutting with an accuracy of no worse than 0.1 mm. The passive elements for both antennas are mounted on brass racks with a diameter of 3 mm and a height of 6 mm. The active exciter is mounted in

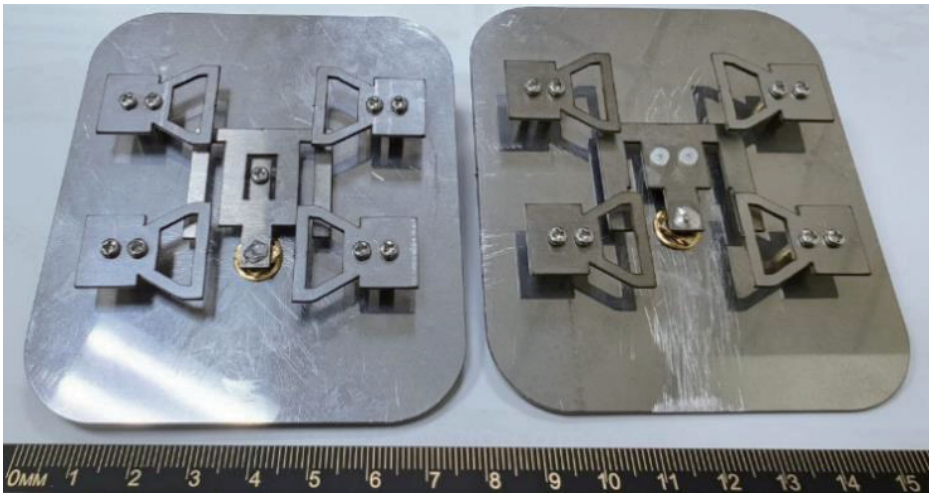

FIGURE 18. The proposed UWB antenna with four single-sided bowtie passive elements and a modified E shaped active exciter mounted with a metal rack (left) and dielectric racks (right).

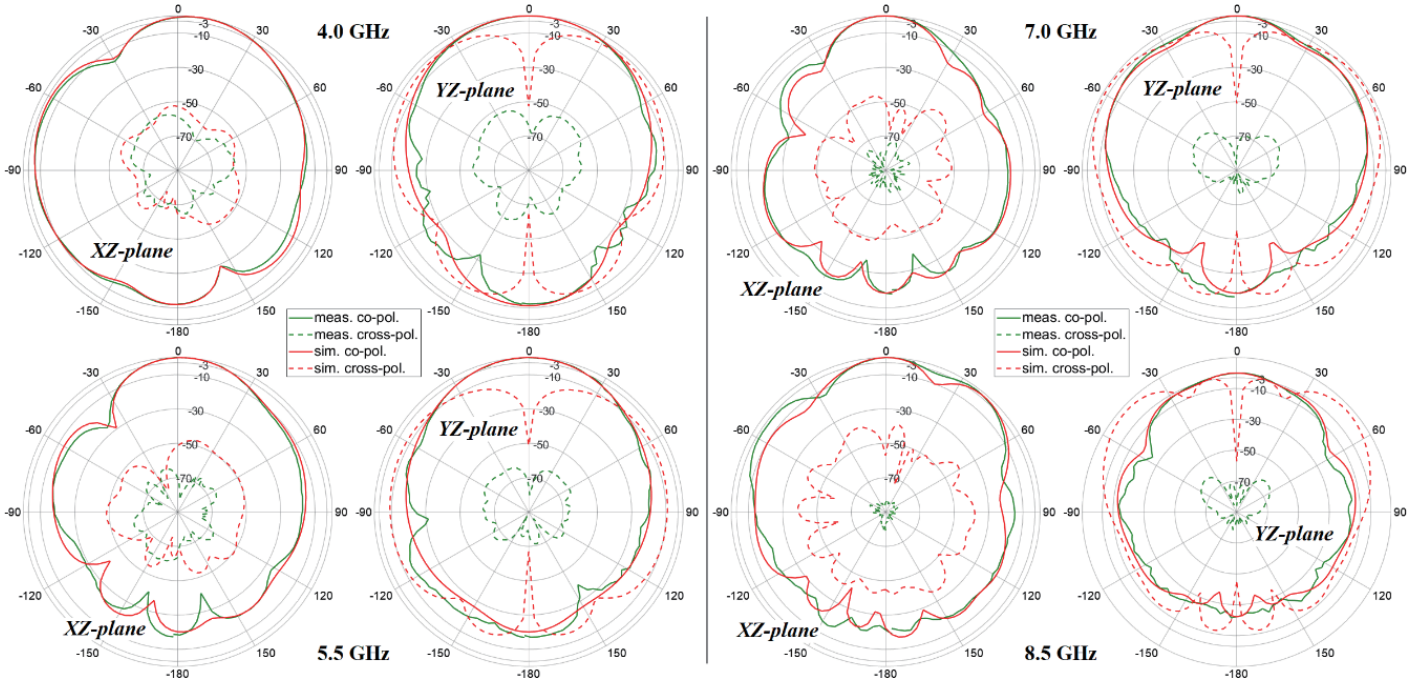

FIGURE 19. The radiation patterns of the proposed ultrawideband antenna with a metal mounting rack under the active exciter.

one case by a brass rack with a diameter of 3 mm and a height of 3 mm; in the second, by two nylon racks, also 3 mm in height. An SMA connector is installed: the outer part is screwed to the ground plane, and the inner conductor is soldered to the input of the active E-shaped exciter.

The measurement results of both antennas are given in Figures 19–22. It is evident from Figures 19 and 20, that the co-polarization RP shapes of both prototypes are close to those obtained from the simulation results, and the measured cross-polarization component in the YZ-plane (H-plane) is much lower than that obtained from the simulation. Both antennas have a symmetrical RP's shape in the YZ plane (H-plane); the maximum is oriented normal to the antenna plane.

According to the measured RPs, the main radiation characteristics of the antenna are determined. The FBR has its lowest value at the lower edge of the operating range and is about 12 dB for both types of antennas; at frequencies from 5–5.5 GHz, the FBR increases to 17 dB or more (similar for both antennas). The measured XPD value in the direction of maximum radiation is not worse than 50 dB; in the main beam region (at half-power beamwidth level, HPBW), XPD does not exceed 40 dB. An antenna with a metal rack under the active exciter provides better XPD. In the YZ plane, in the lower half of the operating range, the HPBW is 50–60° and about 30–40° in the upper half; in the XZ plane, in the lower half of the operating range, the

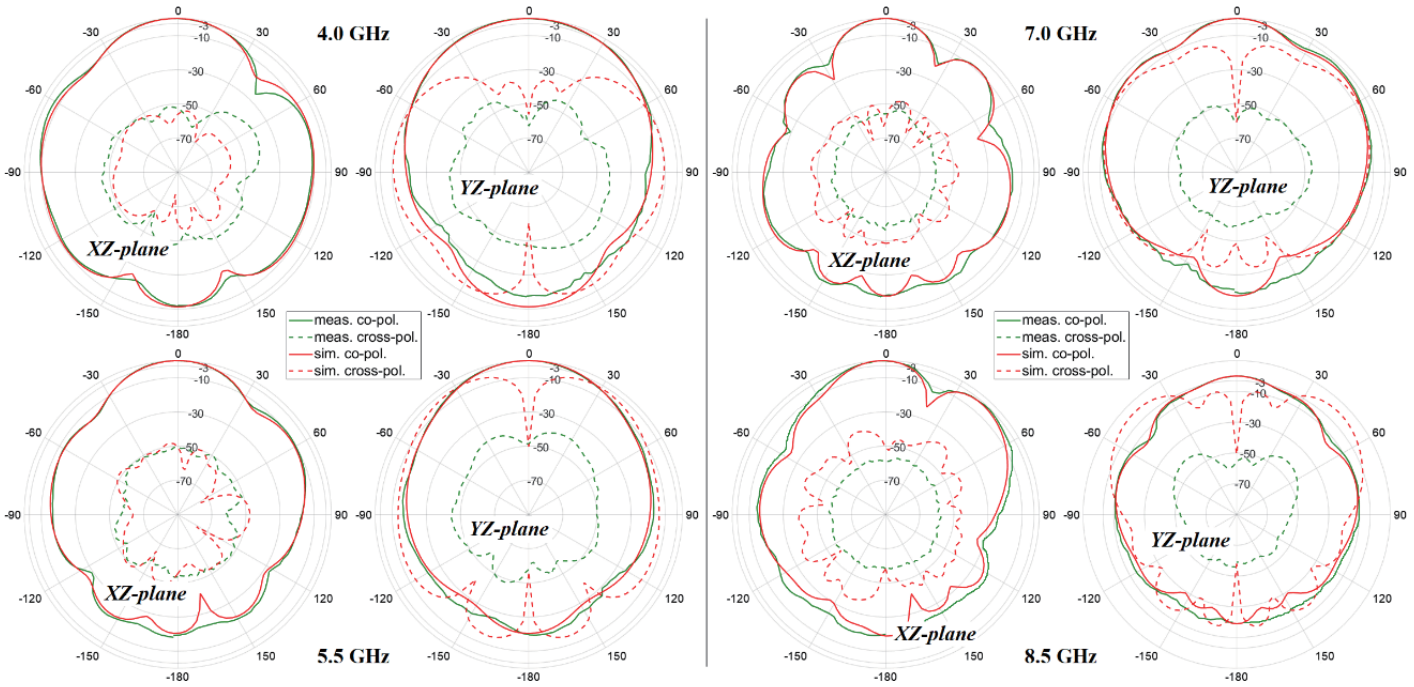

FIGURE 20. The radiation patterns of the proposed ultrawideband antenna with dielectric mounting racks under the active exciter.

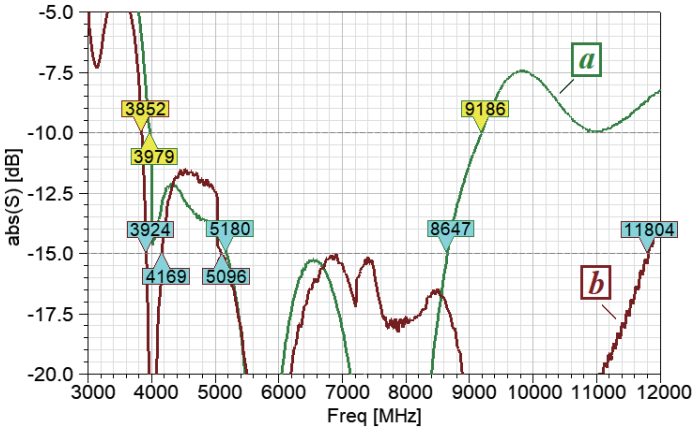

FIGURE 21. The measured reflection coefficient magnitudes of the stacked microstrip antennas with a modified E-shaped active exciter mounted with a metal rack (a) and dielectric racks (b)

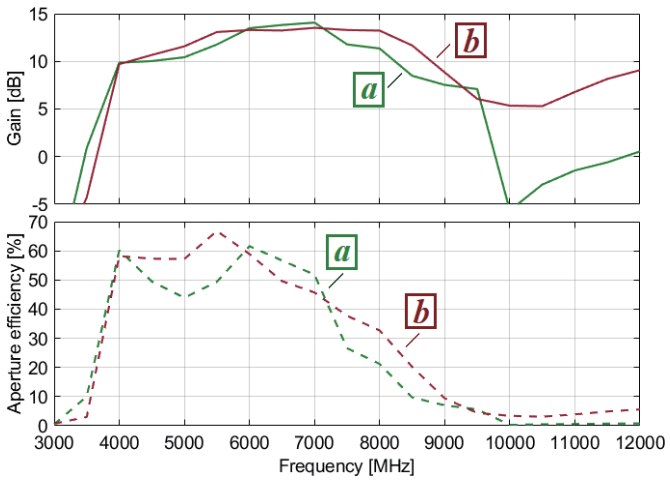

FIGURE 22. The measured gain and aperture efficiency (AE) plots of the stacked microstrip antennas with a modified E-shaped active exciter mounted with a metal rack (a) and dielectric racks (b)

HPBW is about 40–45° and about 30–35° in the upper half for both types of measured antennas.

Figure 21 shows that the antenna with a metal rack has the matching BW of about 79.1% (3979–9186 MHz) with $|S_{11}| \leq -10$ dB and about 50.2% with $|S_{11}| \leq -15$ dB; the antenna with dielectric racks has the matching BW more than 103% (from 3853 MHz to 12 GHz and above) with $|S_{11}| \leq -10$ dB and about 85.5% with $|S_{11}| \leq -15$ dB. The convergence of the measured and simulated plots is quite high; the discrepancies are most likely caused by inaccuracy in the manufacture of the antenna elements.

The antenna patterns and gain measurements were performed in an anechoic chamber. The radiation patterns were evaluated using the general method by direct measurements in the far field of the antenna, using an SMR 20 Rohde & Schwarz generator connected to the antenna under study and a Rohde & Schwarz ESU EMI Test Receiver to measure the power received by the measuring horn UWB antenna. The measured antenna is placed on a rotating stand, as shown in Figure 23.

To determine the antenna gain, an additional reference antenna HF907 Rohde & Schwarz with known characteristics is used. The reference antenna is installed instead of the one being measured, and the received power is measured. Next, knowing

TABLE 1. Comparison between the proposed design and the most effective previous studies in high-gain UWB antennas.

Antenna Type	BW, % ($S_{11} \leq -10$ dB)	BW, % ($S_{11} \leq -15$ dB)	BW, % ($G \geq 10$ dBi)	Gain, dBi (peak / av.)	AE, % (λ_{max}/λ_0)	Overall size λ_{max}/λ_0
Vivaldi antenna loaded with elliptical slots [19]	~ 144.8	–	~ 78.3	~ 11.3 ~ 10.6	–	$1.8 \times 1.3 \times 0.03$ $3.0 \times 2.2 \times 0.05$
Vivaldi antenna with reconfigurable 3D phase adjusting unit lens [20]	~ 100	–	~ 100	~ 13.8 ~ 12.5	–	$1.8 \times 1.04 \times 0.3$ $3.6 \times 2.08 \times 0.6$
Conformal end-fire Vivaldi array [22]	~ 102.5	–	~ 96.9	~ 15.2 ~ 12.6	–	$0.8 \times 0.3 \times 2.5$ $1.6 \times 1.6 \times 4.9$
3D printed horn antenna [30]	~ 72	–	~ 72	~ 14.0 ~ 13.0	~ 60 ~ 60	$1.04 \times 1.3 \times 0.8$ $1.63 \times 2.0 \times 1.25$
Double-ridged horn antenna [31]	~ 184	–	~ 151	~ 15.35 ~ 12.0	~ 29 ~ 3	$2.03 \times 1.3 \times 2.3$ $8.3 \times 5.5 \times 9.3$
Ridged horn antenna with metallic grid sidewalls [32]	~ 181	–	~ 154	~ 17.0 ~ 14.5	~ 80 ~ 21	$1.2 \times 0.8 \times 2.08$ $5.3 \times 3.6 \times 9.06$
Double-ridge horn antenna [33]	~ 161	–	~ 133	~ 18.0 ~ 13.0	~ 28 ~ 6	$2.4 \times 1.2 \times 1.02$ $7.1 \times 3.6 \times 3.05$
2×4 array with an inclined proximity coupled feed [41]	~ 57.2	–	~ 57.2	~ 15.0 ~ 13.2	~ 28 ~ 33	$2.1 \times 1.4 \times 0.09$ $2.8 \times 1.9 \times 0.12$
4×4 aperture coupled microstrip patch antenna array [45]	~ 42.9	–	~ 42.9	~ 21.0 ~ 19.0	~ 50 ~ 68	$2.8 \times 2.9 \times 0.15$ $3.6 \times 3.7 \times 0.19$
E-shaped active exciter and four rectangular passive elements [53]	~ 33.0	~ 26.0	~ 28.8	~ 13.4 ~ 12.2	~ 40 ~ 65	$1.6 \times 1.6 \times 0.1$ $1.4 \times 1.4 \times 0.1$
Modified E-shaped active exciter and four single-sided bowtie passive elements [proposed]	> 103	~ 85.5	~ 77.0	~ 13.5 ~ 12.5	~ 60 ~ 55	$1.05 \times 1.2 \times 0.1$ $1.7 \times 1.9 \times 0.2$

FIGURE 23. The RPs and gain measurement process of the studied stacked microstrip antenna.

the level of the received signal at the antenna under study, the reference antenna and its gain, the gain of the measured antenna at the given frequencies is calculated (Figure 22). To determine the AE values, the equation is used:

$$\eta_{ap} = \frac{\lambda^2}{4\pi \cdot S} G, \tag{9}$$

where λ is the free-space wavelength at the given frequency f; S is the physical area of antenna; G is a measured gain value.

According to Figure 22, the measured antenna gain also corresponds to that obtained in the simulation; an antenna with nylon racks for mounting an active exciter shows the best performance. Table 1 demonstrates the characteristics of the antenna under study in comparison to earlier publications.

6. CONCLUSION

The article provides an overview of ultrawideband antenna technologies and examines modern achievements from both the point of view of omnidirectional and unidirectional antennas. The analysis shows that the best performance among unidirectional UWB antennas is shown by horn and Vivaldi antennas; nonetheless, they have several drawbacks, primarily among them being their large size.

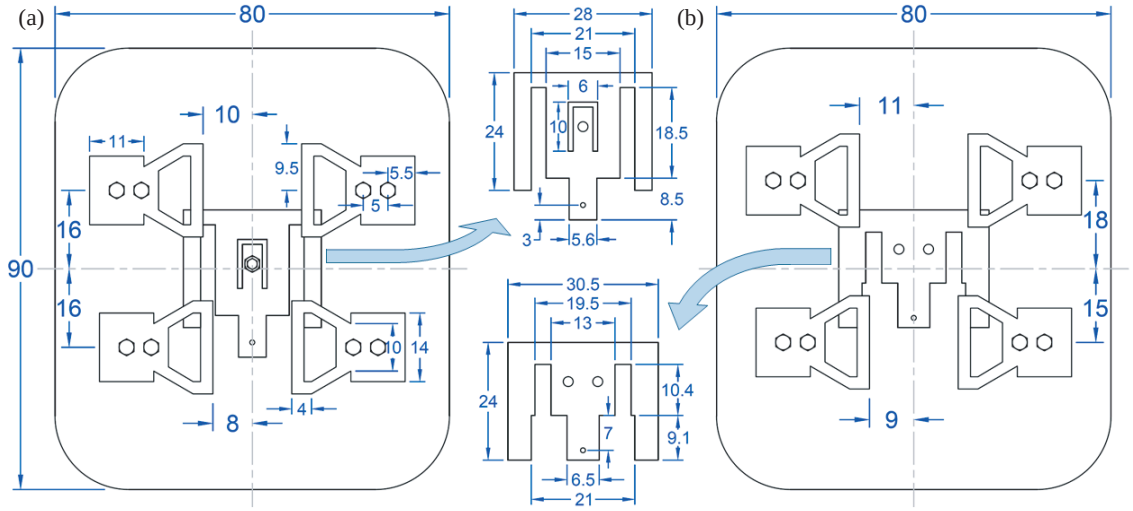

FIGURE 24. The proposed ultrawideband high-gain stacked microstrip antenna with (a) metal and (b) dielectric mounting racks under the modified E-shaped active exciter.

A unique method for expanding the frequency band of a stacked microstrip antenna to an ultrawide one (up to 100%) is proposed. The method consists of using modified E-shaped active and four single-sided bowtie passive exciters, which are attached to the ground plane using racks. Based on the proposed method, an antenna structure was manufactured that has the following characteristics: the matching BW is about 100% with $|S_{11}| \leq -10$ dB and about 85.5% with $|S_{11}| \leq -15$ dB; the usable bandwidth with a gain greater than 10 dBi and XPD greater than 55 dB is about 77%; and the FBR more than 17 dB at frequencies higher than 4.5 GHz. The antenna has small size which is $1.05\lambda_{\max} \times 1.2\lambda_{\max} \times 0.1\lambda_{\max}$ or $1.7\lambda_0 \times 1.9\lambda_0 \times 0.2\lambda_0$.

ACKNOWLEDGEMENT

The author would like to express his sincere thanks to Kseniya Ivanchenko for her diligent proofreading of this paper.

APPENDIX A. PROPOSED ANTENNAS APPEARANCE WITH ITS DIMENSIONS

The appendix contains Figure 24, showing the appearance of the antennas under study with dimensions in millimeters.

REFERENCES

[1] FCC, "Federal communications commission revision of Part 15 of the commission's rules regarding ultra-wideband transmission systems," First Report and Order FCC, 02.V48, 2002.

[2] Hasan, M. N. and M. Seo, "A planar 3.4-9 GHz UWB monopole antenna," in *2018 International Symposium on Antennas and Propagation (ISAP)*, 1–2, Busan, Korea (South), Oct. 2018.

[3] Devana, V. and A. M. Rao, "Design and parametric analysis of beveled UWB triple band rejection antenna," *Progress In Electromagnetics Research M*, Vol. 84, 95–106, 2019.

[4] Ponnapalli, V. L. N. P., S. Karthikeyan, J. L. Narayana, and V. N. K. R. Devana, "A compact novel lamp slotted WLAN band notched UWB antenna integrated with Ku band," *Progress In Electromagnetics Research C*, Vol. 129, 89–98, 2023.

[5] Vinoth, J. C., S. Ramesh, Z. Z. Abidin, S. A. Qureshi, S. Chitra, E. Saranya, M. Josephine, and G. Sneha, "Planar edged UWB antenna for water quality measurement," *Progress In Electromagnetics Research C*, Vol. 130, 83–93, 2023.

[6] Xue, J., A. Ni, L. Liu, Z. Wang, and X. Wang, "An ultra-wideband antenna based on left-handed materials for IoT applications," *Progress In Electromagnetics Research C*, Vol. 140, 151–161, 2024.

[7] Wang, Z., G. Song, W. Nie, M. Yang, C. Li, and M. Wang, "A racket-like UWB MIMO antenna with high isolation," *Progress In Electromagnetics Research C*, Vol. 144, 159–168, 2024.

[8] Park, S. and K.-Y. Jung, "Novel compact UWB planar monopole antenna using a ribbon-shaped slot," *IEEE Access*, Vol. 10, 61 951–61 959, 2022.

[9] Kamma, A., S. R. Gupta, G. S. Reddy, and J. Mukherjee, "Compact UWB ring sectoral monopole antenna with dual polarization," in *2013 Annual IEEE India Conference (INDICON)*, 1–3, Mumbai, India, Dec. 2013.

[10] Ren, J., W. Hu, Y. Yin, and R. Fan, "Compact printed MIMO antenna for UWB applications," *IEEE Antennas and Wireless Propagation Letters*, Vol. 13, 1517–1520, 2014.

[11] Wang, Y., F. Zhu, and S. Gao, "Design of planar ultra-wideband antenna with polarization diversity and high isolation," in *2016 IEEE International Conference on Ubiquitous Wireless Broadband (ICUWB)*, 1–3, Nanjing, China, Oct. 2016.

[12] Divya, S., K. Premchand, and P. H. Krishna, "Arc-shaped monopole antenna with polarization diversity characteristics for UWB applications," in *2017 IEEE International Conference on Power, Control, Signals and Instrumentation Engineering (ICPCSI)*, 1632–1635, Chennai, India, Sep. 2017.

[13] Islam, T., E. M. Ali, W. A. Awan, M. S. Alzaidi, T. A. H. Alghamdi, and M. Alathbah, "A parasitic patch loaded staircase shaped UWB MIMO antenna having notch band for WBAN applications," *Heliyon*, Vol. 10, No. 1, e23711, 2024.

[14] Gibson, P. J., "The Vivaldi aerial," in *1979 9th European Microwave Conference*, 101–105, Brighton, UK, Sep. 1979.

[15] Balanis, C. A., *Antenna Theory: Analysis and Design*, John Wiley & Sons, 2016.

[16] Chen, Z. N., D. Liu, H. Nakano, X. Qing, and T. Zwick, *Handbook of Antenna Technologies*, Springer, 2016.

[17] Dixit, A. S. and S. Kumar, "A survey of performance enhancement techniques of antipodal Vivaldi antenna," *IEEE Access*, Vol. 8, 45 774–45 796, 2020.

[18] Li, K., M. Liu, and H. Zhang, "An L-band ultra wide-band Vivaldi antenna with wide beam angle," in *2020 13th UK-Europe-China Workshop on Millimetre-Waves and Terahertz Technologies (UCMMT)*, 1–3, Tianjin, China, Sep. 2020.

[19] Yin, Z.-F., X.-X. Yang, and T. Lou, "A high gain UWB Vivaldi antenna loaded with elliptical slots," in *2018 International Applied Computational Electromagnetics Society Symposium — China (ACES)*, 1–2, Beijing, China, Aug. 2018.

[20] Sang, L., S. Wu, G. Liu, J. Wang, and W. Huang, "High-gain UWB Vivaldi antenna loaded with reconfigurable 3-D phase adjusting unit lens," *IEEE Antennas and Wireless Propagation Letters*, Vol. 19, No. 2, 322–326, 2020.

[21] Xu, H., J. Lei, C. Cui, and L. Yang, "UWB dual-polarized Vivaldi antenna with high gain," in *2012 International Conference on Microwave and Millimeter Wave Technology (ICMMT)*, Vol. 3, 1–4, Shenzhen, China, May 2012.

[22] Chen, Y., Y. He, W. Li, L. Zhang, S.-W. Wong, and A. Boag, "A 3-9 GHz UWB high-gain conformal end-fire Vivaldi antenna array," in *2021 IEEE International Symposium on Antennas and Propagation and USNC-URSI Radio Science Meeting (APS/URSI)*, 737–738, Singapore, Dec. 2021.

[23] Volakis, J. L. and J. L. Volakis, *Antenna Engineering Handbook*, McGraw-Hill, 2007.

[24] Casula, G. A., P. Maxia, G. Mazzarella, and G. Montisci, "Design of a printed log-periodic dipole array for ultra-wideband applications," *Progress In Electromagnetics Research C*, Vol. 38, 15–26, 2013.

[25] Gowda, E. D. and V. N. Prasad, "Design of log-periodic monopole array patch antenna for UWB applications using alphabetic slots on partial ground plane," in *2020 IEEE International Conference on Electronics, Computing and Communication Technologies (CONECCT)*, 1–5, Bangalore, India, Jul. 2020.

[26] Mistry, K. K., P. I. Lazaridis, Z. D. Zaharis, and T. H. Loh, "Design and optimization of compact printed log-periodic dipole array antennas with extended low-frequency response," *Electronics*, Vol. 10, No. 17, 2044, 2021.

[27] Wang, Q., C. Song, H. Zhou, and L.-Z. Song, "Simulation and analysis of LPFSA loaded with split-ring resonators," in *2019 International Applied Computational Electromagnetics Society Symposium — China (ACES)*, Vol. 1, 1–2, Nanjing, China, Aug. 2019.

[28] Amini, A., H. Oraizi, and M. A. C. zadeh, "Miniaturized UWB log-periodic square fractal antenna," *IEEE Antennas and Wireless Propagation Letters*, Vol. 14, 1322–1325, 2015.

[29] Wang, Z., X. Zhao, F. Ji, S. Huang, and Z. Jiang, "Ultra-wideband cylindrical conformal array antenna based on LP-KDA," in *2020 IEEE MTT-S International Conference on Numerical Electromagnetic and Multiphysics Modeling and Optimization (NEMO)*, 1–4, Hangzhou, China, Dec. 2020.

[30] Midtbøen, V., K. G. Kjelgård, and T. S. Lande, "3D printed horn antenna with PCB microstrip feed for UWB radar applications," in *2017 IEEE MTT-S International Microwave Workshop Series on Advanced Materials and Processes for RF and THz Applications (IMWS-AMP)*, Pavia, Italy, Sep. 2017.

[31] Nan, H., "Design and implementation of high performance UWB horn antenna," in *2018 International Applied Computational Electromagnetics Society Symposium — China (ACES)*, 1–2, Beijing, China, Aug. 2018.

[32] Lin, S., S. Liu, Y. Zhang, and J. Jiao, "Analysis and experiment of a ridged horn antenna with metallic grid sidewalls," *Progress In Electromagnetics Research C*, Vol. 96, 27–41, 2019.

[33] Liu, S., J. Liu, L. Zhao, C. Yuan, N. Hu, and W. Xie, "The design of UWB double-ridge horn antenna," in *2020 9th Asia-Pacific Conference on Antennas and Propagation (APCAP)*, 1–2, Xiamen, China, Aug. 2020.

[34] Qiao, X., H. Zhao, and Z. Jiang, "Wideband and high gain horn antenna with lens and wedge ridge," in *2019 IEEE International Conference on Computational Electromagnetics (ICCEM)*, 1–3, Shanghai, China, Mar. 2019.

[35] Luk, K.-M. and H. Wong, "A new wideband unidirectional antenna element," *International journal of Microwave and Optical Technology*, Vol. 1, No. 1, 35–44, 2006.

[36] Eldek, A. A., "Ultrawideband double rhombus antenna with stable radiation patterns for phased array applications," *IEEE Transactions on Antennas and Propagation*, Vol. 55, No. 1, 84–91, 2007.

[37] Lin, S., X.-Y. Zhang, X.-q. Zhang, X.-y. Zhang, R.-n. Cai, G.-l. Huang, L.-w. Jing, and W.-b. Zhang, "High-gain planar TEM horn antenna fed by balanced microstrip line," in *2011 6th International ICST Conference on Communications and Networking in China (CHINACOM)*, 909–912, Harbin, China, Aug. 2011.

[38] Wei, J., X. Jiang, and L. Peng, "Ultrawideband and high-gain circularly polarized antenna with double-Y-shape slot," *IEEE Antennas and Wireless Propagation Letters*, Vol. 16, 1508–1511, 2017.

[39] Fan, J., J. Lin, J. Cai, and F. Qin, "Ultra-wideband circularly polarized cavity-backed crossed-dipole antenna," *Scientific Reports*, Vol. 12, No. 1, 4569, 2022.

[40] Latha, T., G. Ram, G. A. Kumar, and M. Chakravarthy, "Review on ultra-wideband phased array antennas," *IEEE Access*, Vol. 9, 129 742–129 755, 2021.

[41] Awasthi, A. K., C. D. Simpson, S. Kolpuke, T. D. Luong, J.-B. Yan, D. Taylor, and S. P. Gogineni, "Ultra-wideband patch antenna array with an inclined proximity coupled feed for small unmanned aircraft RADAR applications," *IEEE Open Journal of Antennas and Propagation*, Vol. 2, 1079–1086, 2021.

[42] Johnson, A. D., V. Manohar, S. B. Venkatakrishnan, and J. L. Volakis, "Optimized differential TCDA (D-TCDA) with novel differential feed structure," *IEEE Open Journal of Antennas and Propagation*, Vol. 2, 464–472, 2021.

[43] Li, B., J. Zhang, Y. Deng, and Z. Zhou, "Design of a low-profile ultra-wideband antenna array based on planar dipole elements," in *2018 IEEE Radar Conference (RadarConf18)*, 0125–0128, Oklahoma City, OK, USA, Apr. 2018.

[44] Patwary, A. B. and I. Mahbub, "4 × 4 UWB phased array antenna with >51° far-field scanning range for wireless power transfer application," *IEEE Open Journal of Antennas and Propagation*, Vol. 5, No. 2, 354–367, 2024.

[45] Babaeian, F. and N. C. Karmakar, "4 × 4 element UWB dual-polarized aperture coupled microstrip patch antenna array for chipless rfid," in *2020 IEEE International RF and Microwave Conference (RFM)*, 1–4, Kuala Lumpur, Malaysia, Dec. 2020.

[46] He, D., P. Zhao, and X. Huang, "Novel high gain and compact UWB antenna using multiple radiation arms loaded with rectangular patches," in *2016 IEEE International Conference on Ubiquitous Wireless Broadband (ICUWB)*, 1–3, Nanjing, China, Oct. 2016.

[47] Lakrit, S., H. Medkour, S. Das, B. T. P. Madhav, W. A. E. Ali, and R. P. Dwivedi, "Design and analysis of integrated wilkinson power divider-fed conformal high-gain uwb array antenna with band rejection characteristics for WLAN applications," *Journal of Circuits, Systems and Computers*, Vol. 30, No. 08, 2150133, 2021.

[48] Garbaruk, M., "A planar four-element UWB antenna array with stripline feeding network," *Electronics*, Vol. 11, No. 3, 469, 2022.

[49] Saleh, S., W. Ismail, I. S. Z. Abidin, M. H. Jamaluddin, M. H. Bataineh, and A. Alzoubi, "Simple UWB linear antenna array based on compact Wilkinson and Bagley power dividers," in *2020 IEEE 5th International Symposium on Telecommunication Technologies (ISTT)*, 45–50, Shah Alam, Malaysia, Nov. 2020.

[50] Shishkin, M. S. and S. N. Shabunin, "Analysis of various designs of wideband patch antennas," in *2022 IEEE International Multi-Conference on Engineering, Computer and Information Sciences (SIBIRCON)*, 1190–1193, Yekaterinburg, Russian Federation, Nov. 2022.

[51] Shishkin, M. S., "Wideband high-gain dual-polarized antenna for 5G communications," in *2021 XV International Scientific-Technical Conference on Actual Problems Of Electronic Instrument Engineering (APEIE)*, 311–316, Novosibirsk, Russian Federation, Nov. 2021.

[52] Shishkin, M. S., "Research of a wideband dual-polarization microstrip antenna array on a suspended substrate with irregular arrangement of elements," in *2024 IEEE 25th International Conference of Young Professionals in Electron Devices and Materials (EDM)*, 630–635, Altai, Russian Federation, Jul. 2024.

[53] Shishkin, M. S., "Bandwidth enhancement methods analysis for high-gain stacked microstrip antenna," *Progress In Electromagnetics Research B*, Vol. 107, 19–31, 2024.

[54] Legay, H. and L. Shafai, "New stacked microstrip antenna with large bandwidth and high gain," *IEE Proceedings — Microwaves, Antennas and Propagation*, Vol. 141, No. 3, 199–204, 1994.

[55] Mallahzadeh, A. R., S. E. haghi, and A. Alipour, "Design of an E-shaped MIMO antenna using IWO algorithm for wireless application at 5.8 GHz," *Progress In Electromagnetics Research*, Vol. 90, 187–203, 2009.

[56] Sheik, B. A., P. Sridevi, and P. R. Raju, "E-shaped patch antennas for multitasks/uninterrupted 5G communications," *Wireless Personal Communications*, Vol. 110, No. 2, 873–891, 2020.

[57] Vincenti Gatti, R., R. Rossi, and M. Dionigi, "Single-layer line-fed broadband microstrip patch antenna on thin substrates," *Electronics*, Vol. 10, No. 1, 37, 2021.

[58] Vasekar, A. and M. Mathpati, "Effect of feed point position on metamaterial based patch antenna," *International Journal of Advanced Computational Engineering and Networking*, Vol. 6, No. 7, 33–37, 2018.

[59] Ooi, B. L., M. S. Leong, and Q. Shen, "A novel equivalent circuit for E-shaped slot patch antenna," in *IEEE Antennas and Propagation Society International Symposium. 2001 Digest. Held in conjunction with: USNC/URSI National Radio Science Meeting (Cat. No.01CH37229)*, Vol. 4, 482–485, Boston, MA, USA, Jul. 2001.

[60] Patel, S. K. and Y. P. Kosta, "E-shape microstrip patch antenna design for GPS application," in *2011 Nirma University International Conference on Engineering*, 1–4, Ahmedabad, India, Dec. 2011.

[61] Kumar, D. N., "Multi-technique broadband microstrip patch antenna design," in *International Conference on Applied Physics, Power and Material Science*, Vol. 1172, No. 1, 012112, Telangana, India, Dec. 2018.

[62] Liu, L., C. Zhang, Y. Liu, and Y. Hua, "A high gain and directivity bow tie antenna based on single-negative metamaterial," *Journal of Microwaves, Optoelectronics and Electromagnetic Applications*, Vol. 17, No. 2, 246–259, 2018.

[63] Awl, H. N., Y. I. Abdulkarim, L. Deng, M. Bakır, F. F. Muhammadsharif, M. Karaaslan, E. Unal, and H. Luo, "Bandwidth improvement in bow-tie microstrip antennas: The effect of substrate type and design dimensions," *Applied Sciences*, Vol. 10, No. 2, 504, 2020.

[64] Alsisi, R. H., A. K. Vallappil, and H. A. Wajid, "A metamaterial-based double-sided bowtie antenna for intelligent transport system communications operating in public safety band," *Crystals*, Vol. 13, No. 2, 360, 2023.

[65] Shishkin, M. and S. Shabunin, "Design of a new antenna system for a meteorological radiosonde tracking radar," in *2021 Ural Symposium on Biomedical Engineering, Radioelectronics and Information Technology (USBEREIT)*, 0198–0201, Yekaterinburg, Russia, May 2021.